galaxies

MDPI

Article

Doppler Tomography of the Be Star HD 698

Ilfa A. Gabitova [1], Sergey V. Zharikov [2], Anatoly S. Miroshnichenko [3,4], Alex Carciofi [5], Azamat A. Khokhlov [1,*], Aldiyar Agishev [1] and Peter Prendergast [6]

[1] Faculty of Physics and Technology, Al-Farabi Kazakh National University, Al-Farabi Ave., 71, Almaty 050040, Kazakhstan; ilfa3110@gmail.com (I.A.G.); aldiyar.agishev@gmail.com (A.A.)
[2] Instituto de Astronomía, Universidad Nacional Autónoma de México, AP 106, Ensenada 22800, Baja California, Mexico; zhar@astro.unam.mx
[3] Department of Physics and Astronomy, University of North Carolina–Greensboro, Greensboro, NC 27402, USA; a_mirosh@uncg.edu
[4] Fesenkov Astrophysical Institute, Observatory, 23, Almaty 050020, Kazakhstan
[5] Instituto de Astronomia, Geofísica e Ciências Atmosféricas, Universidade de São Paulo, Rua do Matão 1226, Cidade Universitária, São Paulo 05508-900, SP, Brazil; carciofi@usp.br
[6] Kernersville Observatory, Winston-Salem, NC 27285, USA
* Correspondence: kh.azamat92@gmail.com

Abstract

We present a Doppler tomography study of the Be star HD 698, recently resolved via interferometry as a post-mass-transfer binary system consisting of a Be star and a stripped, pre-subdwarf companion. Based on 76 high-resolution optical spectra obtained between 2014 and 2023, we analyze the Hα and Hβ emission lines and apply Doppler tomography to map the structure of the circumstellar disk. The Hα line reveals an asymmetric, multi-component velocity distribution, with an emission feature closely following the orbital motion of the companion. V/R variations in both Hα and Hβ lines are phase-locked with the companion's orbital motion, indicating a tidally induced disk asymmetry. We discuss possible origins of the companion-centered Hα emission, including a circumsecondary disk, a transient mass-transfer stream, and stellar wind.

Keywords: spectroscopy; Doppler tomography; binary stars; Be stars; circumstellar matter

check for updates

Received: 20 May 2025
Revised: 9 July 2025
Accepted: 14 July 2025
Published: 16 July 2025

Citation: Gabitova, I.A.; Zharikov, S.V.; Miroshnichenko, A.S.; Carciofi, A.; Khokhlov, A.A.; Agishev, A.; Prendergast, P. Doppler Tomography of the Be Star HD 698. *Galaxies* **2025**, *13*, 80. https://doi.org/10.3390/galaxies13040080

Copyright: © 2025 by the authors. Licensee MDPI, Basel, Switzerland. This article is an open access article distributed under the terms and conditions of the Creative Commons Attribution (CC BY) license (https://creativecommons.org/licenses/by/4.0/).

1. Introduction

Classical Be stars are rapidly rotating B-type stars, typically in or near the main sequence, that exhibit Balmer-line emission originating from a circumstellar gaseous decretion disk [1]. These stars generally rotate at 70–80% of their breakup velocity and expel material that forms a Keplerian disk around the equator through mechanisms not yet fully understood such as non-radial pulsations or localized magnetic fields [2]. Over time, this material evolves under viscous forces into a relatively stable flattened disk.

The presence of ionized gas in the disk accounts for the emission lines and infrared excess typical of Be stars and also contributes to their photometric and spectroscopic variability. Emission lines often exhibit double-peaked profiles with alternating asymmetries or violet-to-red (V/R) peak intensity variations, believed to be caused by one-armed density waves precessing in the disk [3,4]. V/R cycles may span several years in isolated stars or be modulated by a companion's gravitational influence in binary systems, leading to orbital-phase-locked asymmetries [5]. The complex behavior of Be-star disks has been extensively reviewed, e.g., [2,6], establishing these stars as valuable test cases for disk physics around rapidly rotating stars.

A significant fraction of classical Be stars may exist in binary systems, e.g., [7,8]. There are population studies that support this as well, e.g., [9–11]. At the same time, there are Be/X-ray binaries with neutron star companions accreting from the Be disk [12]. Recent attention has been focused on systems that are not obvious X-ray sources, but rather are suspected to contain compact objects or evolved stars that are difficult to detect optically. Notable examples include LB-1, initially reported as a Be star orbiting a $\sim$70 $M_\odot$ black hole with an orbital period of 79 days [13], but later reinterpreted as a Be star with a stripped helium-star (pre-subdwarf) companion of lower mass [14]. Similarly, HR 6819 was proposed as a Be/black hole binary, but was subsequently resolved as a Be star with a pre-subdwarf companion, with no black hole present [15–17]. These findings support a scenario in which some classical Be stars are the products of past binary mass transfer. The currently observed Be star was spun up by accreting mass, while the original more massive star was stripped of its envelope, becoming a pre-subdwarf with a narrow-lined spectrum. In LB-1 and HR 6819 systems, the pre-subdwarf was initially mistaken for a main-sequence B star due to its temperature and luminosity, and its large RV semi-amplitude led to the erroneous conclusion that it was orbiting a massive, invisible companion. It was later recognized that the visible star was in fact a low-mass, evolved object orbiting the Be star.

Detecting companions in such systems at ultraviolet, optical, and infrared wavelengths remains difficult, as they often produce only weak spectral and photometric signatures. The Be star typically dominates the optical spectrum, and the high flux contrast makes it difficult to detect narrow spectral features from a faint companion. Compact companions such as neutron stars or black holes are detectable only indirectly—via X-ray emission or through dynamical mass estimates based on the Be star's radial velocity (RV). Historically, large mass functions from single-lined orbital solutions and occasional chemical anomalies (e.g., nitrogen enhancement) served as indirect evidence for unseen companions [18]. Only recently, with high-sensitivity spectroscopy, ultraviolet observations, and optical interferometry, has it become feasible to directly characterize these secondaries.

The focus of this study is HD 698 (V742 Cas), a classical Be star long suspected of hosting a massive, unseen companion. Initially identified as a single-lined spectroscopic binary by Pearce [19], its orbital period of approximately 56 days was confirmed by subsequent work [20,21]. Sahade et al. [22] conducted a detailed analysis of IUE ultraviolet spectra, determining a period of 55.9 days with a nearly circular orbit and an RV semi-amplitude $K \approx 80\,km\,s^{-1}$. The derived mass function of $3.10\,M_\odot$ indicated that, even for an edge-on geometry, the unseen companion must exceed $\sim 8\,M_\odot$, so its spectral invisibility could only be reconciled with a neutron star, black hole, or a sub-luminous star contributing little to the observed spectrum. HD 698 was therefore included in the Chochol & Mayer catalog of B stars with high mass functions and undetected companions [18]. However, unlike typical Be X-ray binaries, HD 698 lacks strong X-ray emission or photometric signatures from the companion.

Rivinius et al. [23] recently conducted a detailed interferometric and spectroscopic study of HD 698, resolving the system as a low-contrast binary and mapping its astrometric orbit. Using CHARA interferometry in the H-band, they spatially separated the two components with a measured angular semi-major axis of 0.663 ± 0.003 mas. Their analysis showed that the brighter H-band source is the stripped pre-subdwarf companion, which dominates the absorption spectrum and exhibits CNO-processed abundances. The Be star, likely the fainter component in the near-infrared, contributes mainly through emission features. Given this updated understanding of HD 698's architecture, an important step is to investigate whether the Be star's disk exhibits signs of gravitational perturbation by the stripped pre-subdwarf companion. In Be binaries, the companion may induce disk asymmetries or drive a phase-locked two-armed density wave [24].

Doppler tomography, introduced by Marsh and Horne [25], is a powerful technique used to study such effects, combining time-resolved spectra covering the binary orbit and reconstructing a two-dimensional velocity-space map of the emitting regions. This technique has been successfully applied in other systems; for example, Zharikov et al. [26] analyzed π Aquarii and identified a non-uniform Hα emission ring with an orbitally modulated density enhancement. Similarly, Gabitova et al. [27] employed Doppler tomography to study the evolution of the disk around κ Draconis during a dissipation event.

In this work, we apply Doppler tomography to the HD 698 system using a continuous set of optical spectra (Section 2). We analyze V/R variations in Hα and Hβ lines and their correlation with RV shifts in absorption lines (Section 3). In Section 4, we discuss the disk structure and implications for the binary dynamics. Conclusions and directions for future research are presented in Section 5.

2. Observations and Data Reduction

This study was based on a total of 76 échelle spectra obtained with the spectral resolution of $R \sim$12,000. The dataset included 69 spectra collected between 2014 and 2023 at the Three College Observatory (TCO) using a 0.81-m telescope equipped with a fiber-fed échelle spectrograph covering the wavelength range ∼3900–7900 Å. In addition, 7 spectra were obtained at the Kernersville Observatory (KO) between 2016 and 2018 using a 0.5-m telescope and an échelle spectrograph with a smaller wavelength range of 4175–7900 Å.

Individual exposures ranged from 480 to 900 s, with each final spectrum composed of 3–5 combined exposures. Typical signal-to-noise ratios in the continuum near the Hα line ranged from 100 to 150 in the final spectra. The spectra covered all orbital phases of the system.

Data reduction was carried out using the IRAF echelle package. Wavelength calibration was completed with thorium–argon (ThAr) comparison lamp spectra. More details about data reduction procedures can be found in [28]. All reduced spectra were interpolated to a uniform step size of $\Delta\lambda = 0.1$ Å. In the Hα region, telluric absorption features were removed by applying humidity-dependent template profiles generated through a Gaussian interpolation of individual telluric lines.

3. Spectral Analysis

We measured RVs of the absorption lines in the 4450–4545 Å region using the cross-correlation technique, implemented via the IRAF xcsao task. The spectra were first continuum-normalized and corrected to the heliocentric frame.

The RV curve was fitted with a sinusoidal model using the curve_fit function from the scipy package (v1.15.2, https://scipy.org, accessed on 15 April 2025). Based on the results of Rivinius et al. [23] and Gabitova et al., in preparation [29], we adopted the interpretation that these RVs reflect the orbital motion of the narrow-lined companion. Consequently, we defined phase zero as the inferior conjunction of the companion star for the purpose of correct positioning of the binary's star components in Doppler tomography maps.

We also examined the V/R variability of the Hα and Hβ lines. The Hβ emission profile appears as a double-peaked structure superimposed on a broad absorption feature. In contrast, the Hα line exhibits a complex morphology: the double-peaked profile is partially obscured by a superposed narrow, single-peaked emission component that varies in phase with the absorption-line RV curve. This additional component likely originates near the same narrow-lined companion.

To isolate the disk-related emission in Hα, we subtracted a Gaussian component with a fixed FWHM of 3.0 Å and peak intensity of 0.3. The Gaussian was Doppler-shifted using the sinusoidal RV curve derived from the absorption lines. While one-peaked Gaussian does not account for the complex behavior of Hα's strongest emission, it qualitatively improves the symmetry of the Doppler map of the Hα line (see Section 4) and allows for V/R measurements that follow the expected behavior of a double-peaked emission line.

We measured the V/R ratio in both Hα (after correction) and Hβ lines by calculating the ratio of emission peak maxima relative to the local continuum. To compute the V/R ratio, we identified the local maxima on either side of the central dip in each emission profile. For Hβ, the peaks were measured directly from the double-peaked emission feature. For Hα, the V and R peaks were measured after subtraction of the narrow central component, which otherwise obscures the disk-related emission; in profiles where the peaks remained blended or ambiguous, no V/R ratio was computed. Both Hα and Hβ V/R variations were fitted with sinusoidal models using the curve_fit function and we found no significant phase shift between them.

Both Hα and Hβ exhibit V/R variations that are phase-locked with the orbital motion (see Figure 1), as demonstrated in Figure 2. In typical Be binaries, where the companion contributes little to the total optical flux, such phase-locked V/R behavior is generally interpreted as evidence for tidal interactions inducing disk asymmetries, e.g., [5], such as a two-armed spiral or a phase-locked density enhancement. However, in the case of HD 698, due to the significant optical flux contribution from the pre-subdwarf companion, its absorption features in Balmer lines can significantly affect the observed emission-line morphology. Since the narrow absorption was not subtracted prior to measuring the V/R ratio, part of the observed variability could arise from the absorption feature moving through the emission line profile, artificially lowering the peak intensity where it overlaps. This effect can mimic phase-locked V/R variations even in a non-perturbed disk. Therefore, while genuine disk asymmetry remains a plausible interpretation, we cannot exclude the alternative explanation that the observed modulation is partially or primarily due to the orbital motion of the companion's absorption.

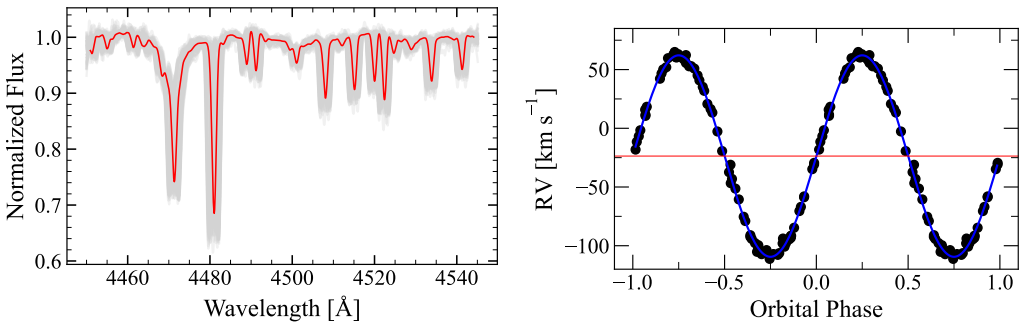


Figure 1. (**Left**) Profile of the cross-correlation region averaged over 76 individual spectra. (**Right**) RV curve of the absorption lines in the 4450–4545 Å region, folded with the orbital period. Average error of the measurements is equal to 1.7 km s^{-1}. The blue line shows the sinusoidal fit; the red horizontal line marks the RV of the mass center.

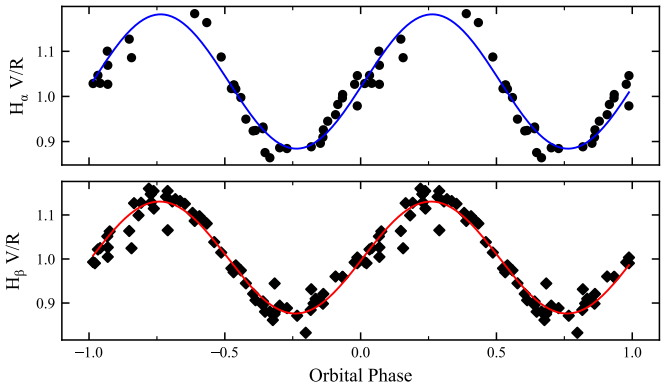


Figure 2. (**Top**) V/R variations of the Hα line, measured after subtracting the narrow emission component, folded with the orbital period. The blue line shows sinusoidal fit. (**Bottom**) V/R variations of the Hβ line, folded with the orbital period. The red line shows sinusoidal fit. In both cases, no correction was applied for the companion's Hα and Hβ absorption.

4. Doppler Tomography

To investigate the structure and kinematics of the emitting regions in the HD 698 system, we performed Doppler tomography using the dopmap program [30]. Doppler maps were generated for the Hα (with both the raw and the narrow emission component corrected), the Hβ emission lines (Figure 3, right panels, from top to bottom), and the Cr II (4824 Å) absorption (Figure 4). The left panels in Figure 3 show averaged line profiles and the middle panels demonstrate phase-resolved spectra repeated twice for clarity.

The plus signs on the maps correspond to positions of the system components, while the cross corresponds to the position of the center of mass of the system ($V_x = 0$ km s^{-1}, $V_y = 0$ km s^{-1}). The Be star is located at $V_x = 0$ km s^{-1}, $V_y = -12.78$ km s^{-1}, while the companion is located at $V_x = 0$ km s^{-1}, $V_y = 85.19$ km s^{-1}. Roche lobes for both stars were calculated using Eggleton's formula [31]. The positions were calculated using the orbital parameters listed in Table 1 and are consistent with the measured RV semi-amplitude $K_2 = 85.80 \pm 0.40$ km s^{-1}, demonstrating good precision. The inclination angle was derived by [23]. The mass ratio used for positioning the components in the Doppler maps is based on the RV semi-amplitude of the Be star (K_1), which was derived directly from the same set of spectra and will be presented in a forthcoming analysis (Gabitova et al., in preparation [29]).

Table 1. Orbital parameters of the HD 698 binary system.

Parameter	Value
P [days]	55.928 ± 0.003
T_0 [HJD]	$2{,}456{,}778.940 \pm 0.197$
γ [km s^{-1}]	-23.66 ± 0.30
K_2 [km s^{-1}]	85.80 ± 0.40
M_1 [M$_\odot$]	7.3 ± 0.2
M_2 [M$_\odot$]	1.1 ± 0.2
$q = M_1/M_2$	6.8 ± 0.8
i [degrees]	60.6 ± 0.3

Parameters listed are as follows: P—orbital period; T_0—epoch of the inferior conjunction of the companion star; γ—systemic velocity; K_2—semi-amplitude of the RV variations of the companion star; M_1—mass of the Be star; M_2—mass of the pre-subdwarf companion; q—mass ratio, defined as M_1/M_2; i—inclination angle.

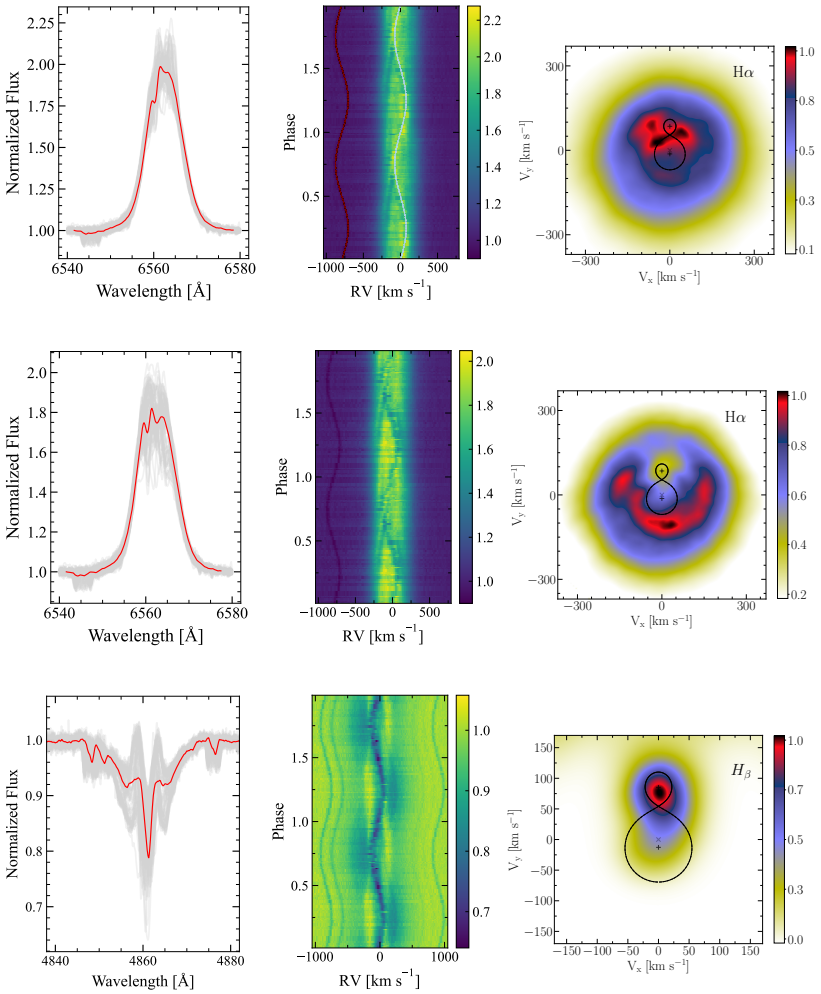


Figure 3. (**Left panels**) Average line profiles (red) overlaid on individual spectra (gray). (**Middle panels**) Phase-resolved spectra. (**Right panels**) Doppler tomograms of the Hα and Hβ lines. The top row corresponds to raw Hα emission spectra, while the middle row shows spectra from which the narrow Hα emission component was subtracted. The bottom row corresponds to Hβ absorption spectra, analyzed using inverted spectra to produce a Doppler tomogram. The white sinusoidal line in the top middle panel traces the RV curve of the narrow Hα emission component, which coincides with the motion of the companion as shown on the 6548 Å N II absorption line (dark red line).

The Doppler map of the original Hα line displays a complex, multi-component structure. One of the prominent features roughly follows the RV curve of the stripped companion, suggesting a possible origin near the secondary. To isolate this component, we subtracted a single-peaked Gaussian profile with fixed FWHM and amplitude, Doppler-shifted using the companion's RV curve. This subtraction is model-dependent; it does not represent a physical decomposition of the line but rather a simplifying assumption aimed at exploring the residual disk morphology. After subtraction of the extra emission component (as described in Section 3), the Hα map reveals a more regular, torus-like structure centered at $V_x = 41.1$ km s^{-1}, $V_y = -105.1$ km s^{-1}. This emission is concentrated on the side of the disk facing away from the companion and might arise from the fainter, trailing arm of the two-armed spiral in a tidally disturbed disk. The emission maximum shows a slight offset, likely due to residual contamination, as the subtraction could not perfectly isolate the companion-related emission.

It should be noted that single-peaked Gaussian does not effectively account for the complex behavior we observe in the Hα line profiles. Phase-resolved spectra of the Hα

line shown in Figure 3 reveal a localized feature that does not follow a sinusoidal motion. It appears on the blue wing of the Hα line at phase $\sim$0.25. In phases 0.6–1.0, it moves along the component associated with the companion, enhancing its emission. The weaker emission spot we see on the original Hα Doppler map with the center at $V_x = -63.2$ km s^{-1}, $V_y = 90.4$ km s^{-1} likely corresponds to this unusual source. The elongated region associated with the companion appears over-subtracted on the right side, where sinusoidal motion is not enhanced, while on the left side, residuals remain after subtraction.

The Hβ map was constructed using inverted spectra, treating absorption dips as if they were emission features. The resulting map shows a more concentrated peak intensity spot centered near $V_x = 3.1$ km s^{-1}, $V_y = 77.1$ km s^{-1}, consistent with the RV amplitude of the stripped companion. This confirms that the dominant Hβ absorption originates in the pre-subdwarf. However, the feature is elongated in the direction of the Be star, suggesting an additional contribution, likely from broad, low-level absorption in the Be star's photosphere. While Hβ also contains weak emission below the continuum, visible in the line profile, this is not clearly recovered in the inverted map.

The phase-resolved spectrum of Hβ demonstrates two notable features beyond dominant absorption from the companion. First, broad absorption appears at phases $\sim$0.25 and $\sim$0.75 in the outer wings of the line. This absorption follows orbital motion of the companion with a bigger amplitude. Second, the Hβ line shows emission peaks that appear to vary in counter-phase to the RVs of the absorption lines. This behavior could be expected if the emission originates near the Be star, whose orbital motion is opposite to that of the companion. However, as discussed in Section 3, the observed phase-locked modulation may be partially or even dominantly driven by the companion's absorption, rather than by genuine disk asymmetry.

To validate the interpretation that the absorption spectrum belongs to the companion, we applied the same Doppler inversion method to the Cr II absorption line. As shown in Figure 4, the absorption peak maps precisely to the expected position of the companion star in velocity space, confirming the consistency of our orbital solution.

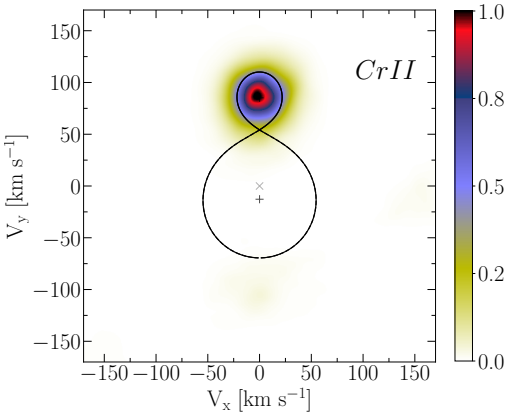


Figure 4. Doppler map of the 4824 ÅCr II absorption line.

5. Discussion

5.1. Origin of the Companion-Related Emission Component

The Doppler tomograms of HD 698's Hα line reveal an extra emission feature coincident with the orbital velocity of the companion. One plausible interpretation is a circumsecondary accretion disk around the companion. Recent high-resolution SPH simulations by Rubio et al. [24] demonstrated that in Be binary systems, gravitational interaction causes mass from the Be disk to enter the companion's Roche lobe, where it forms an

accretion disk around the companion. This circumsecondary disk is present in models across a wide range of orbital periods, mass ratios, and disk viscosities.

In interacting binaries, the mass-gaining star can host an accretion disk that contributes to Balmer line emission. For example, in some Algol-type systems, the hot primary is surrounded by a transient accretion disk that produces Hα emission, e.g., [32]. In Be X-ray binaries, a neutron star or black hole companion may capture material from the Be star's decretion disk, forming a temporary accretion disk (as proposed in systems like MWC 656), though at low accretion rates and X-ray quiescence [33]. By analogy, HD 698's companion, although not massive, is extremely bloated and could host a small disk or envelope that emits Hα.

An alternative explanation is emission from a gas stream through the inner Lagrange point (L1). In classic semi-detached binaries, the Roche-lobe overflow stream can produce line emission en route to the accretor, often manifesting as an "S-wave" or a distinct feature in Doppler maps, where tomographic studies of interacting systems have indeed detected Hα emission along the ballistic stream trajectory [34]. For HD 698, which is not an obvious Roche-lobe overflow system, a continuous L1 stream is not expected under normal conditions. However, if the Be disk extends to or beyond the Roche lobe boundary, a transient overflow or mass-transfer stream could occur. Hα emission from this stream would appear near the L1's velocity in velocity space, as seen in the top panel Doppler map in Figure 3.

A third possibility is a stellar wind or outflow from the companion. If the companion is a hot, luminous star (or if it is accreting at a low level), it might drive a weak Hα-emitting wind. Emission from a circumbinary outflow or a photoionized region around the companion could contribute an Hα component that roughly tracks the companion's motion. For example, Doppler tomography of the cataclysmic variable AY Psc revealed low-velocity Hα emission attributed to a disk wind or outflow region in addition to the usual disk features [34]. In HD 698, although the companion is luminous, we expect it to be a bloated, stripped star (Gabitova et al., in preparation [29]) , with a lower effective temperature than typical subdwarf companions in Be binaries, making the stellar wind scenario unlikely.

Both L1 streams and companion outflows are occurrences known to happen in compact binaries, such as cataclysmic variables (CVs). These interpretations must be applied to HD 698 with caution. The physical scale of the HD 698 system is much larger and its orbital velocities are lower than in CVs, so any mass-transfer or wind phenomena will be correspondingly more diffuse. In CVs, orbital periods of hours lead to Keplerian disk speeds of hundreds of km s^{-1} and tightly bound accretion structures, whereas HD 698's 56-day orbit involves velocities in the order of only a few tens of km s^{-1}. Features that appear as distinct components in a CV's Doppler map would be subtle and smeared out in a long-period B-star binary. Nonetheless, the presence of this extra Hα emission in HD 698 is a strong indicator of some form of binary interaction that warrants further investigation.

In addition to the emission component coincident with the companion's motion, the residual Hα emission observed after subtraction reveals an asymmetric distribution centered on the side of the disk opposite the companion. This morphology is consistent with tidally induced distortions, such as a two-armed spiral structure, which naturally arise in Be binaries due to the companion's gravitational influence [24]. Additionally, localized heating or photoionization of the inner disk face by the hot stripped companion may potentially amplify emission on the side facing the companion.

5.2. Limitations of Doppler Tomography

Before drawing conclusions about the spatial structure of the HD 698 system, it is important to consider the assumptions and limitations inherent to Doppler tomography. The tomographic reconstruction method (as introduced by Marsh and Horne [25]) assumes that the observed line profiles can be described by a static distribution of emitters in velocity space.

This implies that the emission distribution is constant over the orbital cycle and that all motion is confined to the orbital plane, an assumption "clearly violated in many cases" [35]. For instance, any time variability in the Hα emission will tend to blur or smear out features in the Doppler map [35]. In HD 698, the Be disk's V/R variability indicates that the emission structure evolves over time. Our tomogram represents an orbital average of the dataset and may smear out transient or non-repeating features that do not remain fixed in the rotating frame.

Doppler tomography inherently produces a velocity-space image; translating this to a real-space picture requires assuming a kinematic model. For a purely Keplerian disk, the mapping from real space to velocity space is relatively straightforward—one finds that each physical location in the disk corresponds to a point in the Doppler map rotated by 90° (since the velocity vector is perpendicular to the radius in circular Keplerian orbits) [25]. If there is gas on non-Keplerian trajectories (radial infall, outflows, or standing in the co-rotating frame), its emission will not align with the simple disk interpretation.

These limitations mean that while our Doppler tomograms demonstrate companion-centric Hα emission, the interpretation is not unique. We have explored plausible scenarios above, but determining whether the dominant contribution arises from a circumsecondary disk or a localized stream requires additional evidence beyond the tomographic intensity distribution alone.

6. Conclusions & Future Work

In summary, we have investigated the Be binary HD 698 (V742 Cas) using Doppler tomography of its Hα and Hβ emission lines. We identified an Hα emission component coincident with the RVs of the companion star. This could be a signature of material associated with the companion, a faint accretion disk or gas stream from L1 point overflow. The residual disk morphology observed in Hα is consistent with emission from a tidally distorted, possibly spiral structure. Irradiation effects from the stripped companion may also influence disk brightness asymmetries. Given the complex appearance of Hα in HD 698, it is likely that multiple emission sources coexist, and no single interpretation can be uniquely favored without detailed radiative transfer modeling.

We also observe V/R variability in the Balmer lines, phase-locked with the orbital period, a pattern previously interpreted in other systems as evidence of tidally induced disk asymmetry. However, since the stripped star in HD 698 contributes significantly to the optical continuum, the observed modulation could partially or primarily result from the absorption line crossing through the emission profile. While we cannot rule out the presence of a tidally induced disk structure, we emphasize that the current data do not uniquely support that scenario. Detailed modeling and absorption correction are needed to disentangle geometric effects from line-profile contamination.

These findings make HD 698 an important case study of disk–companion interaction in a Be binary system. A more detailed, quantitative modeling of the HD 698 system is underway (Gabitova et al., in preparation [29]). In that forthcoming analysis, we will attempt to reproduce the observed spectroscopic and photometric properties through radiative transfer modeling.

Beyond that, smoothed-particle hydrodynamic (SPH) modeling of a Be star disk in the gravitational field of a companion would help to verify the mechanisms proposed here. Such simulations have been successfully used in other Be binaries to demonstrate the effects of the companion star on the Be disk, such as the formation of spiral arms or oscillation modes and even the formation of a circumsecondary accretion disk [24,36].

On the observational side, we will continue monitoring the optical region of HD 698 over many orbital cycles. This will allow us to perform phase-resolved tomography and even modulation tomography that accounts for variability, thereby separating truly stationary features from those that change with the orbital phase.

Author Contributions: Conceptualization, I.A.G., S.V.Z. and A.S.M.; Software, A.A.; Formal analysis, I.A.G. and A.S.M.; Investigation, I.A.G. and S.V.Z.; Data curation, A.S.M. and P.P.; Writing—original draft, I.A.G. and A.A.K.; Writing—review and editing, S.V.Z., A.S.M. and A.C.; Visualization, I.A.G.; Project administration, A.A.K. All authors have read and agreed to the published version of the manuscript.

Funding: This research was funded by the Science Committee of the Ministry of Education and Science of the Republic of Kazakhstan (Grant No. AP19175392). S.V.Z. acknowledges the DGAPA-PAPIIT grant IN119323.

Data Availability Statement: Original spectra reported in this study are available upon request from the A.S.M. via email at a_mirosh@uncg.edu.

Acknowledgments: This research has made use of the SIMBAD database, operated at CDS, Strasbourg, France, SAO/NASA ADS.

Conflicts of Interest: The authors declare no conflicts of interest.

Abbreviations

The following abbreviations are used in this manuscript: RV—radial velocity; IRAF—Image Reduction and Analysis Facility; FWHM—full width at half-maximum; V/R—violet-to-red peak intensity ratio in a double-peaked emission-line profile; R—spectral resolving power; EW—equivalent width; TCO—Three College Observatory.

References

1. Jaschek, M.; Egret, D. Catalog of Be stars. In *Be Stars*; Jaschek, M., Groth, H.G., Eds.; D. Reidel Publishing Company: Dordrecht, The Netherlands, 1982; Volume 98, p. 261.
2. Rivinius, T.; Carciofi, A.C.; Martayan, C. Classical Be stars. Rapidly rotating B stars with viscous Keplerian decretion disks. *Astron. Astrophys. Rev.* **2013**, *21*, 69. [CrossRef]
3. Kato, S. Low-frequency, one-armed oscillations of Keplerian gaseous disks. *Publ. Astron. Soc. Jpn.* **1983**, *35*, 249–261. [CrossRef]
4. Okazaki, A.T. Long-Term V/R Variations of Be Stars Due to Global One-Armed Oscillations of Equatorial Disks. *Publ. Astron. Soc. Jpn.* **1991**, *43*, 75–94. [CrossRef]
5. Miroshnichenko, A.S.; Chari, R.; Danford, S.; Prendergast, P.; Aarnio, A.N.; Andronov, I.L.; Chinarova, L.L.; Lytle, A.; Amantayeva, A.; Gabitova, I.A.; et al. Searching for Phase-Locked Variations of the Emission-Line Profiles in Binary Be Stars. *Galaxies* **2023**, *11*, 83. [CrossRef]
6. Porter, J.M.; Rivinius, T. Classical Be Stars. *Publ. Astron. Soc. Pac.* **2003**, *115*, 1153–1170. [CrossRef]
7. Miroshnichenko, A.S. A statistical study of galactic bright Be stars. In *Active OB Stars: Structure, Evolution, Mass Loss, and Critical Limits*; Neiner, C., Wade, G., Meynet, G., Peters, G., Eds.; Cambridge University Press: Cambridge, UK, 2011; Volume 272, pp. 304–305. [CrossRef]
8. Nazé, Y.; Rauw, G.; Czesla, S.; Smith, M.A.; Robrade, J. Velocity monitoring of γ Cas stars reveals their binarity status. *Mon. Not. R. Astron. Soc.* **2022**, *510*, 2286–2304. [CrossRef]
9. Boubert, D.; Evans, N.W. On the kinematics of a runaway Be star population. *Mon. Not. R. Astron. Soc.* **2018**, *477*, 5261–5278. [CrossRef]
10. Gies, D.R. Be Stars: Single and Binary Components. In *The Influence of Binaries on Stellar Population Studies*; Vanbeveren, D., Ed.; Springer: Dordrecht, The Netherlands, 2001; pp. 95–110. [CrossRef]

11. Hastings, B.; Langer, N.; Wang, C.; Schootemeijer, A.; Milone, A.P. Stringent upper limit on Be star fractions produced by binary interaction. *Astron. Astrophys.* **2021**, *653*, A144. [CrossRef]
12. Reig, P. Be/X-ray binaries. *Astrophys. Space Sci.* **2011**, *332*, 1–29. [CrossRef]
13. Liu, J.; Zhang, H.; Howard, A.W.; Bai, Z.; Lu, Y.; Soria, R.; Justham, S.; Li, X.; Zheng, Z.; Wang, T.; et al. A wide star-black-hole binary system from radial-velocity measurements. *Nature* **2019**, *575*, 618–621. [CrossRef]
14. Shenar, T.; Bodensteiner, J.; Abdul-Masih, M.; Fabry, M.; Mahy, L.; Marchant, P.; Banyard, G.; Bowman, D.M.; Dsilva, K.; Hawcroft, C.; et al. The "hidden" companion in LB-1 unveiled by spectral disentangling. *A&A* **2020**, *639*, L6. [CrossRef]
15. Bodensteiner, J.; Shenar, T.; Mahy, L.; Fabry, M.; Marchant, P.; Abdul-Masih, M.; Banyard, G.; Bowman, D.M.; Dsilva, K.; Frost, A.J.; et al. Is HR 6819 a triple system containing a black hole? An alternative explanation. *A&A* **2020**, *641*, A43. [CrossRef]
16. El-Badry, K.; Quataert, E. A stripped-companion origin for Be stars: Clues from the putative black holes HR 6819 and LB-1. *Mon. Not. R. Astron. Soc.* **2021**, *502*, 3436–3455. [CrossRef]
17. Frost, A.J.; Bodensteiner, J.; Rivinius, T.; Baade, D.; Merand, A.; Selman, F.; Abdul-Masih, M.; Banyard, G.; Bordier, E.; Dsilva, K.; et al. HR 6819 is a binary system with no black hole. Revisiting the source with infrared interferometry and optical integral field spectroscopy. *A&A* **2022**, *659*, L3. [CrossRef]
18. Chochol, D.; Mayer, P. Binaries with Invisible Massive Components. In *Exotic Stars as Challenges to Evolution*; Tout, C.A., van Hamme, W., Eds.; Astronomical Society of the Pacific: San Francisco, CA, USA, 2002; Volume 279, p. 143.
19. Pearce, J.A. The coexistence of stellar and interstellar calcium lines in the massive B9 star H. D. 698. *Mon. Not. R. Astron. Soc.* **1932**, *92*, 877. [CrossRef]
20. Hutchings, J.B.; Bernard, J.E. A spectroscopic reinvestigation of the massive binary HD 698. *Publ. Astron. Soc. Pac.* **1978**, *90*, 179–183. [CrossRef]
21. Sahade, J. The spectroscopic binary HD 698. *Obs. Astron. Plata Sep. Astron.* **1967**, *77*, 219.
22. Sahade, J.; Barba, R.; Kondo, Y. The Orbital Parameters and the IUE Spectrum of the Single-lined Spectroscopic Binary HD 698. *APJ Suppl. Ser.* **1992**, *81*, 303. [CrossRef]
23. Rivinius, T.; Klement, R.; Chojnowski, S.D.; Baade, D.; Abdul-Masih, M.; Przybilla, N.; Guarro Fló, J.; Heathcote, B.; Hadrava, P.; Gies, D.; et al. Newborn Be star systems observed shortly after mass transfer. *A&A* **2025**, *694*, A172. [CrossRef]
24. Rubio, A.C.; Carciofi, A.C.; Bjorkman, J.E.; de Amorim, T.H.; Okazaki, A.T.; Suffak, M.W.; Jones, C.E.; Candido, P.P. High-spatial-resolution simulations of Be star disks in binary systems: I. Structure and kinematics of coplanar disks. *arXiv* **2025**, arXiv:2502.11626. [CrossRef]
25. Marsh, T.R.; Horne, K. Images of accretion discs—II. Doppler tomography. *Mon. Not. R. Astron. Soc.* **1988**, *235*, 269–286. [CrossRef]
26. Zharikov, S.V.; Miroshnichenko, A.S.; Pollmann, E.; Danford, S.; Bjorkman, K.S.; Morrison, N.D.; Favaro, A.; Guarro Fló, J.; Terry, J.N.; Desnoux, V.; et al. Doppler tomography of the circumstellar disk of π Aquarii. *A&A* **2013**, *560*, A30. [CrossRef]
27. Gabitova, I.A.; Miroshnichenko, A.S.; Zharikov, S.V.; Amantayeva, A.; Khokhlov, S.A. Doppler Tomography of the Circumstellar Disk of the Be Star κ Draconis. *Galaxies* **2024**, *12*, 23. [CrossRef]
28. Miroshnichenko, A.S.; Danford, S.; Andronov, I.L.; Aarnio, A.N.; Lauer, D.; Buroughs, H. Refining Orbits of Bright Binary Systems. *Galaxies* **2023**, *11*, 8. [CrossRef]
29. Gabitova, I.A.; de Amorim, T.; Carciofi, A.; Miroshnichenko, A.S.; Zharikov, S.V.; Prendergast, P.; Agishev, A.T.; Khokhlov, S.A. *HD 698: Radiative Transfer Modeling of an Early Post-Mass-Transfer Be Binary*; Al-Farabi Kazakh National University: Almaty, Kazakhstan. 2025; *manuscript in preparation*.
30. Spruit, H.C. Fast maximum entropy Doppler mapping. *arXiv* **1998**, arXiv:astro–ph/9806141. [CrossRef]
31. Eggleton, P.P. Aproximations to the radii of Roche lobes. *APJ* **1983**, *268*, 368–369. [CrossRef]
32. Olson, E.C.; Etzel, P.B. Rapid H(alpha) Emission Variations in Accretion Disks in Long-Period ALGOLS. *AJ* **1995**, *109*, 1308. [CrossRef]
33. Zamanov, R.K.; Stoyanov, K.A.; Marchev, D.; Tomov, N.A.; Wolter, U.; Bode, M.F.; Nikolov, Y.M.; Stefanov, S.Y.; Kurtenkov, A.; Latev, G.Y. Optical spectroscopy of the Be/black hole binary MWC 656 - interaction of a black hole with a circumstellar disc. *Astron. Nachrichten* **2022**, *343*, e24019. [CrossRef]
34. Kára, J.; Zharikov, S.; Wolf, M.; Amantayeva, A.; Subebekova, G.; Khokhlov, S.; Agishev, A.; Merc, J. The Z Camelopardalis-type Star AY Piscium: Stellar and Accretion Disk Parameters. *APJ* **2023**, *950*, 47. [CrossRef]
35. Steeghs, D. Doppler tomography of accretion in binaries. *Astron. Nachrichten* **2004**, *325*, 185–188. [CrossRef]
36. Rast, R.G.; Jones, C.E.; Carciofi, A.C.; Suffak, M.W.; Fonseca Silva, A.C.; Henry, G.W.; Tycner, C. Evolution of the Disk in the Be Binary δ Scorpii Probed during Three Periastron Passages. *APJ* **2024**, *968*, 30. [CrossRef]

Disclaimer/Publisher's Note: The statements, opinions and data contained in all publications are solely those of the individual author(s) and contributor(s) and not of MDPI and/or the editor(s). MDPI and/or the editor(s) disclaim responsibility for any injury to people or property resulting from any ideas, methods, instructions or products referred to in the content.